12-1-2020

Biglycan and chondroitin sulfate play pivotal roles in bone toughness via retaining bound water in bone mineral matrix

Rui Hua

Qingwen Ni
Texas A and M International University

Travis D. Eliason
Southwest Research Institute

Yan Han
The University of Texas at San Antonio

Sumin Gu

See next page for additional authors

Biglycan and chondroitin sulfate play pivotal roles in bone toughness via retaining bound water in bone mineral matrix

Rui Hua [a], Qingwen Ni [c], Travis D. Eliason [d], Yan Han [b], Sumin Gu [a], Daniel P. Nicolella [d], Xiaodu Wang [b] and Jean X. Jiang [a]

***a* - Department of Biochemistry and Structural Biology,** *UT Health, San Antonio, TX, USA*
***b* - Department of Mechanical Engineering,** *University of Texas at San Antonio, TX, USA*
***c* - Department of Physics,** *Texas A&M International University, Laredo, TX, USA*
***d* - Department of Materials Engineering,** *Southwest Research Institute, San Antonio, TX, USA*

Corresponding authors. ***Xiaodu.Wang@utsa.edu*****,*** ***jiangj@uthscsa.edu*****.***
https://doi.org/10.1016/j.matbio.2020.09.002

Abstract

Recent *in vitro* evidence shows that glycosaminoglycans (GAGs) and proteoglycans (PGs) in bone matrix may functionally be involved in the tissue-level toughness of bone. In this study, we showed the effect of biglycan (Bgn), a small leucine-rich proteoglycan enriched in extracellular matrix of bone and the associated GAG subtype, chondroitin sulfate (CS), on the toughness of bone *in vivo*, using wild-type (WT) and *Bgn* deficient mice. The amount of total GAGs and CS in the mineralized compartment of *Bgn* KO mouse bone matrix decreased significantly, associated with the reduction of the toughness of bone, in comparison with those of WT mice. However, such differences between WT and *Bgn* KO mice diminished once the bound water was removed from bone matrix. In addition, CS was identified as the major subtype in bone matrix. We then supplemented CS to both WT and *Bgn* KO mice to test whether supplemental GAGs could improve the tissue-level toughness of bone. After intradermal administration of CS, the toughness of WT bone was greatly improved, with the GAGs and bound water amount in the bone matrix increased, while such improvement was not observed in *Bgn* KO mice or with supplementation of dermatan sulfate (DS). Moreover, CS supplemented WT mice exhibited higher bone mineral density and reduced osteoclastogenesis. Interestingly, *Bgn* KO bone did not show such differences irrespective of the intradermal administration of CS. In summary, the results of this study suggest that Bgn and CS in bone matrix play a pivotal role in imparting the toughness to bone most likely *via* retaining bound water in bone matrix. Moreover, supplementation of CS improves the toughness of bone in mouse models.

Introduction

Osteoporosis and bone fragility fractures are a major concern of health care for our rapidly growing aging population. Although the current common consensus is that the fracture risk is mainly dependent on bone mineral density (BMD) [1], more recent evidence shows that BMD alone lacks sensitivity to evaluate the mechanical performance of bone accurately [2–4]. This is likely, in part, because bone is a hierarchical composite of mineralized type I collagen fibrils embedded in a matrix of non-collagenous proteins (NCPs) and hydroxyapatite mineral phase [5]. In the past, extensive efforts have been made to study the contribution of the mineral and collagen phases to the mechanical competence of bone [6–10]. It was not until recently that the direct effect of NCPs on bone mechanical properties has started to attract more attention [11–13]. Proteoglycans (PGs) are a set of the structural NCPs in bone extracellular matrix, which have strong affinity to both collagen and mineral crystals [14,15]. Typically, PGs contain glycosaminoglycans (GAGs) chains, which are long unbranched polysaccharides comprising a series of repeating disaccharide unit, attached to core proteins [16]. GAGs are highly negatively

charged, thus possessing a great osmotic potential to attract water into the matrix, while matrix water has been reported to function as a critical mediator to facilitate the plastic deformation of bone at both bulk and ultrastructural levels [17−22]. However, the role of PGs and GAGs in regulating mechanical behavior of bone remains poorly investigated [23].

Our previous *in vitro* studies using human cadaveric bone samples showed that PGs and GAGs might play an important role in sustaining bone toughness *via* retaining bound water in the matrix [24,25]. The studies also showed that loss of chondroitin sulfate (CS), a major subtype of GAGs in bone matrix, was associated with age-related deterioration of bone toughness. It has been reported that biglycan (Bgn) is a major subtype of CS-containing PGs and is highly expressed in bone tissues [26−28]. Bgn has two Ser-Gly attachment sites in the N-terminal region and belongs to the class I type small leucine-rich PGs (SLRPs), which are characterized by relatively small protein cores (36-42 kDa) harboring tandem leucine rich repeats [29−31].

The current understanding of effects of Bgn on bone is mainly focused on its biological aspects. Studying mice with targeted *Bgn* disruption has revealed the involvement of Bgn in the regulation of postnatal skeletal growth. *Bgn* deficiency may lead to decreases in bone mass, bone mineral density, long bone length, and bone biomechanical strength compared to age-matched controls [32]. Histological analysis indicates that *Bgn* KO mice may have less trabecular volume and thinner cortices. *Bgn* deletion may cause structural abnormalities of bone collagen fibrils and impair the metabolic activity of bone marrow stromal cells (BMSCs) [33,34]. However, it is still unclear whether *Bgn* depletion *in vivo* would lead to loss of bound water in bone matrix and subsequently result in deterioration of bone toughness.

The aim of this study was to investigate the specific role of Bgn in retaining bound water in bone matrix and maintaining bone toughness using a *Bgn*-deficient mouse model. Biochemical, biophysical, and biomechanical experiments were performed to determine the amount of total GAGs, CS and bound water in bone matrix, and their effects on the tissue-level toughness of bone. In addition, this study investigated the effect of matrix Bgn on the efficacy of supplemental CS in improving bone toughness *in vivo* using the mouse model.

Results

Biglycan deficiency induces reduction of total glycosaminoglycans in bone matrix

PGs isolated from bone matrix of 6-month-old WT and *Bgn* KO mice were subjected to Western blotting analysis using an anti-Bgn antibody. The Bgn protein band under both glycosylated (Fig. 1A) and deglycosylated (Fig. 1B) conditions can be detected in the mineralized bone lysates of WT mice, with a Bgn protein band shift observed after the treatment by deglycosylation enzyme mix to remove both N-linked and O-linked glycans. Compared to WT samples, the expression of Bgn was abolished in both non-treated and deglycosylated groups of *Bgn* knockout (KO) mice, with comparable amount of total protein loaded on the gel as shown by Ponceau S staining (Fig. 1A and B, left panels). Consistently, immunohistochemistry staining of Bgn protein in paraffin sections prepared from WT and *Bgn* KO mice showed that the expression of Bgn was abundant in cell bodies of osteocytes in WT mice (Fig. 1C, left panel, black arrows), while only background signal could be detected in the sections from *Bgn* KO mice (Fig. 1C, middle panel). Rabbit IgG was used as an isotype control (Fig. 1C, right panel), showing no reactivity.

We next examined whether there would be a reduction of the GAGs amount induced by *Bgn* deficiency, as Bgn is one of the major PGs in bone matrix that contain the GAGs [27,28,35]. The level of total GAGs was determined by DMMB assay in both mineralized and non-mineralized compartments of bone. Consistent with our previous observations in human bone study [24], GAGs were mainly present in the mineralized portion of mouse bone matrix. Compared with WT mice, *Bgn* KO mice showed a significant decrease in total GAGs amount in the mineralized matrix, while the difference was not evident in the non-mineralized compartment (Fig. 1D). To further validate the GAGs changes under *Bgn* deficiency condition, bone sections prepared from the mid-diaphysis of WT and *Bgn* KO mice were stained with Alcian blue. The stained GAGs were visible around the osteocytes and throughout the lacunar-canalicular network in bone matrix (Fig. 1E, left panel). Quantification of the Alcian blue staining by integrating the intensity over of the area of interest indicated a significant reduction of GAGs content in *Bgn* KO mice (Fig. 1E, right panel). These results suggest that amount of total GAGs in bone matrix decreases with the loss of *Bgn* in bone matrix.

Biglycan deficiency decreases amount of bound water and bone toughness

The coupling effect of proteoglycans and bound water in maintaining bone toughness has been shown in human bone during the aging process [24,25]. To examine the effects of *Bgn* deficiency on the amount of bound water, cortical bone lysates of WT and *Bgn* KO mice were analyzed by low-energy NMR measurements. Results showed that the index of bound water was 0.55±0.02 in

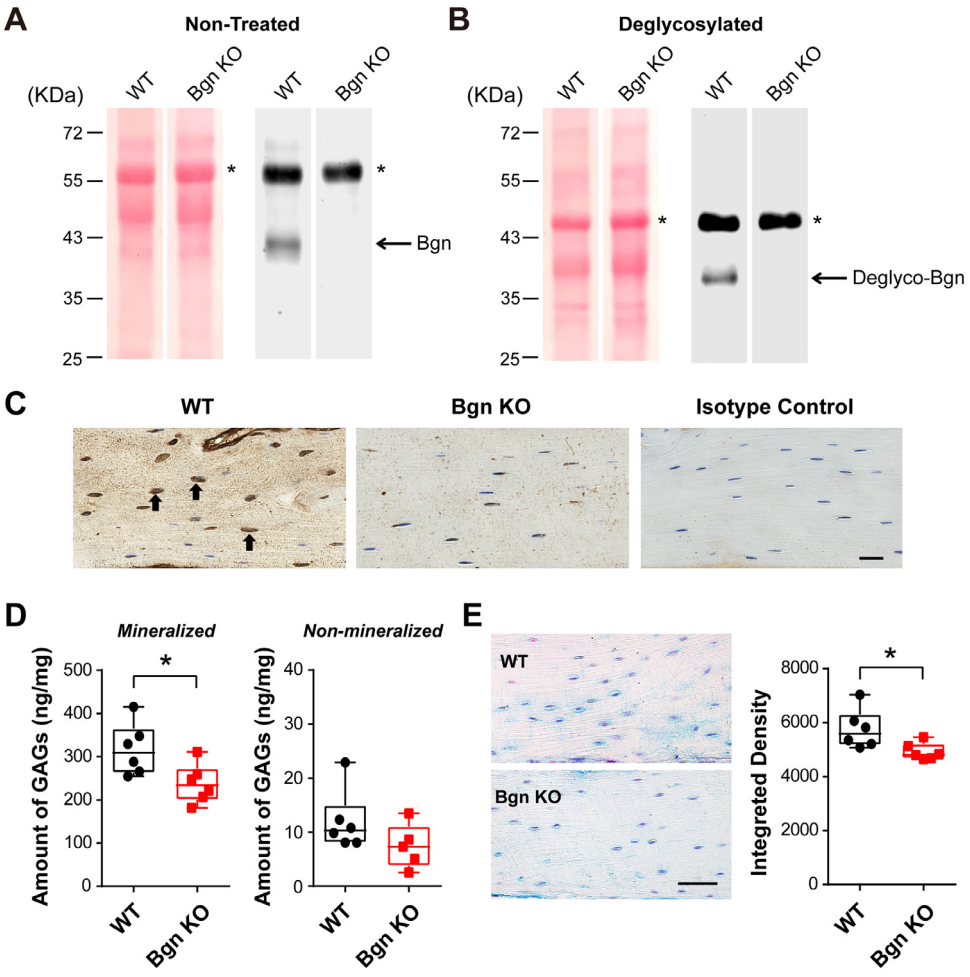

Fig. 1. *Bgn* KO mice showed decreased amount of total GAGs in bone. (A) Proteoglycans from WT and *Bgn* KO mice mineralized bone matrix were analyzed by western blots probed with anti-Bgn antibody (right panel). Ponceau S staining showed comparable sample loading from WT and *Bgn* KO mice (left panel). The asterisk (*) denotes non-specific bands. (B) Proteoglycans from WT and *Bgn* KO mice mineralized bone matrix were treated with deglycosylation enzyme mix to reveal the Bgn core protein, and were analyzed by western blots probed with anti-Bgn antibody (right panel). Ponceau S staining showed comparable sample loading from WT and *Bgn* KO mice (left panel). The asterisk (*) denotes non-specific bands. (C) Paraffin sections of femoral cortical bone from WT (left panel) and *Bgn* KO mice (middle panel) were immunolabeled with anti-Bgn antibody. The positive signals (brown) were labeled by black arrows. Rabbit IgG was used as isotype control (right panel). Scale bar, 20 μm. (D) The total GAGs amount from mineralized (left panel) and non-mineralized (right panel) compartments of WT and *Bgn* KO mice bone matrix was quantified by DMMB assay. (E) WT and *Bgn* KO mice paraffin-embedded bone tissue sections were stained with Alcian blue (left panel). Scale bar, 50 μm. The integrated density of the staining was analyzed by NIH Image J software (right panel). n = 5-6. * $p < 0.05$.

WT mice bone, and 0.48±0.02 in *Bgn* KO mice, exhibiting a significant reduction in bound water in bone matrix (Fig. 2A). We next investigated the tissue-level toughness determined by nanoscratch test using bone samples from the mid-diaphyseal femurs of WT and *Bgn* KO groups. Under the wet condition, in which the samples were soaked in PBS solution during the test, the tissue-level toughness of bone decreased significantly for *Bgn* KO mice compared to WT mice (Fig. 2B). However, under the dry condition, in which the bound water in bone matrix was removed by heating, the change in the tissue-level toughness induced by *Bgn* deficiency was totally abolished. In addition, dehydration had a profound effect on the toughness of WT bone when comparing between the wet and dry conditions. Noticeably, *Bgn* KO mice also showed reduction of tissue-level toughness after dehydration, indicating the potential involvement of other factors in retaining water in the bone. Taken together, we concluded that Bgn is one of the PGs in bone mineral matrix that plays a key role in retaining water and sustaining the toughness of bone.

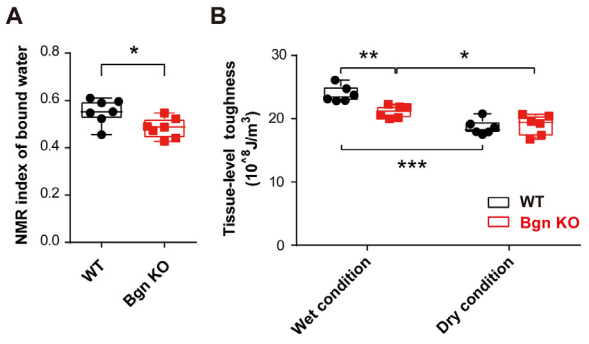

Fig. 2. *Bgn* KO mice showed decreased amount of bound water and bone toughness. (A) The amount of bound water in WT and *Bgn* KO mice bone matrix was measured by low-field NMR. (B) The femoral cortical samples from WT and *Bgn* KO mice were subjected to a nano-scratch test for tissue-level toughness at mid-diaphysis. Bone toughness was determined under wet (normal) condition and dry bone condition with dehydration to remove the bound water in bone matrix. n = 6-7. * $p < 0.05$; ** $p < 0.01$; *** $p < 0.001$.

Chondroitn sulfate is the major glycosaminoglycan subtype in bone mineral matrix and is decreased under biglycan deficiency condition

GAGs extracted from WT mice bone mineralized matrix were analyzed by agarose gel electrophoresis. In addition, the *in situ* visualization of GAGs was realized *via* toluidine blue staining. Pure heparin sulfate (HS), dermatan sulfate (DS) and CS were served as standard controls. WT mice bone showed a single band of GAGs aligned with the CS population (Fig. 3A). Chondroitinase ABC specifically degrades CS and DS by catalyzing the eliminative degradation of polysaccharides containing (1-4)-β-D-hexosaminyl and (1-3)-β-D-glucuronosyl or (1-3)-α-L-iduronosyl linkages to disaccharides containing 4-deoxy-β-D-gluc-4-enuronosyl groups. After chondroitinase ABC digestion, bands of CS, DS and GAGs isolated from mouse bone disappeared, further suggesting that the majority of GAGs in mineralized matrix is in the form of CS.

In order to determine the change of CS band intensity under *Bgn* deficiency condition, GAGs from both non-mineralized (non-M) and mineralized compartments of WT and *Bgn* KO mice bone were analyzed by agarose gel electrophoresis. GAGs from equal weight of bone samples were loaded on the gel. There were no detectable GAG forms in the non-mineralized portion in both the WT and *Bgn* KO mice bone matrix (Fig. 3B, left panel). Densitometry measurements revealed that CS band intensity was significantly lower in the *Bgn* KO mice than in the WT mice (Fig. 3B, right panel), suggesting that *Bgn* deficiency may lead to decrease of CS in bone matrix.

Chondroitin sulfate supplement improves GAGs and bound water amount, tissue-level toughness, and bone mineral density in WT mice, but not in *Bgn* KO mice

We have previously reported that GAGs amount decreases with aging and is associated with deterioration of bone toughness in human cadaveric bone samples [24]. Considering that CS is the major form of GAGs in bone and *Bgn* depletion may lead to a decreased toughness of the tissue, we investigated if supplementing CS *in vivo* would improve the toughness of middle-aged mice bone. Based on the life phase equivalencies between mouse and

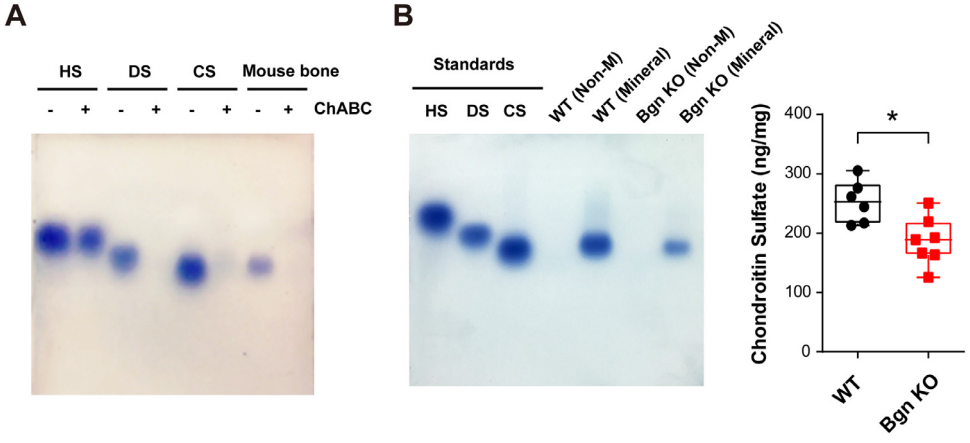

Fig. 3. Chondroitin sulfate is identified as a major GAG subtype in the mineral matrix of mouse bone and is reduced in *Bgn* KO mice. (A) Agarose gel electrophoresis showed various subtypes of GAGs, heparin sulfate (HS), dermatan sulfate (DS), and chondroitin sulfate (CS). GAGs extracted from WT mouse bone matrix were examined and confirmed by chondroitinase ABC digestion. (B) GAGs from non-mineralized (Non-M) and mineralized (Mineral) compartments of WT and *Bgn* KO mice bone matrix were analyzed by agarose gel electrophoresis. CS was detected in mineralized bone matrix (left panel). The CS band intensity was quantified by NIH Image J software (right panel). n = 6-7. * $p < 0.05$.

human, we selected middle-aged mice around 10 to 11-month-old for CS supplementation study. We administrated CS intradermally at the base of the mouse tail, since a previous study has reported intradermal injection of CS and its incorporation into mouse tissues [36]. CS (European pharmacopoeia reference standard) was injected once a week for 4 weeks. The amount of GAGs in mineralized and non-mineralized cortical bone matrix of both WT and *Bgn* KO mice was determined.

The results showed that supplementation of CS significantly increased the GAGs amount in the mineralized portion of WT bone matrix; while the GAGs amount in non-mineralized matrix of WT bone was not affected when compared with saline controls (Fig. 4A). Interestingly, administration of CS appeared to have no effect on the amount of GAGs in both non-mineralized and mineralized bone matrix for *Bgn* KO mice (Fig. 4E). We next examined the level of bound water from both WT and *Bgn* KO mice bones treated with saline or CS. As shown in Fig. 4B, compared to saline control group, supplementation of CS significantly increased the amount of bound water in WT mice. In contrast, the *Bgn* KO mice did not exhibit any difference of bound water amount after CS injection (Fig. 4F).

We then measured the tissue-level toughness of bone for WT and *Bgn* KO mice with CS or saline injections by the nanoscratch test. The results showed a significant improvement of bone toughness in WT mice supplemented with CS compared to controls with saline injection (Fig. 4C). However, no difference existed in the tissue-level toughness between CS and saline injected *Bgn* KO mice (Fig. 4G). These results further suggested the importance of GAGs in retaining bound water and conferring tissue-level toughness into the bone. The whole-body total bone mineral density (BMD) was determined before and after saline or CS injection. A significant elevation of BMD was observed in the WT mice injected with CS compared with those injected with saline alone (Fig. 4D), while the *Bgn* KO group did not exhibit any significant BMD increase after CS supplementation (Fig. 4H).

Further, we tested whether other types of GAGs would have a similar effect on bone in WT mice.

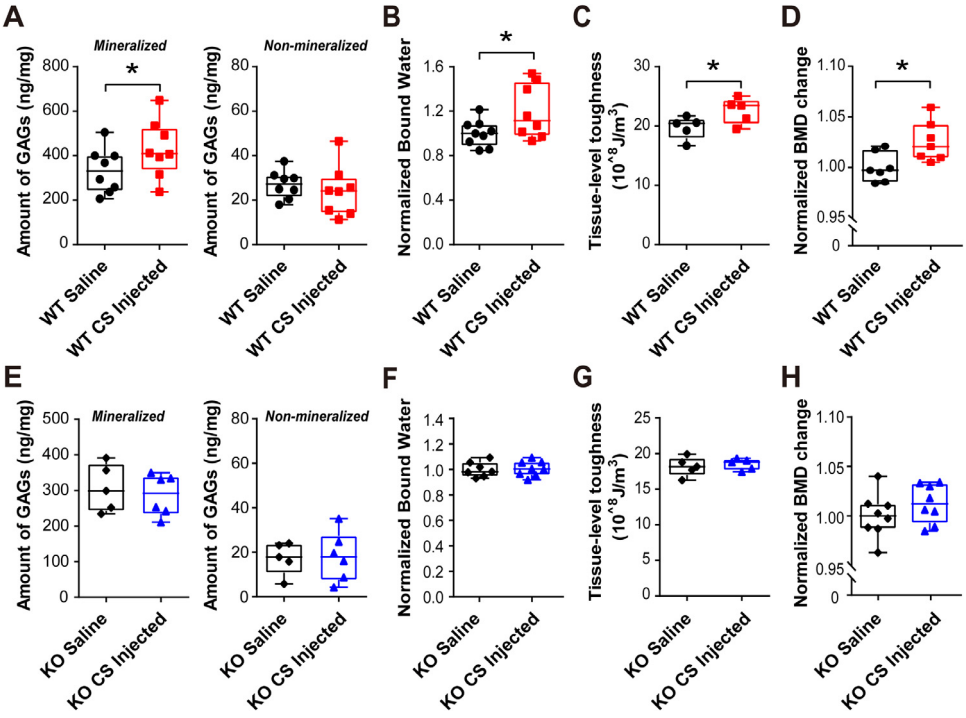

Fig. 4. Chondroitin sulfate supplementation improved GAGs amount, bone mineral density (BMD) and tissue-level toughness in WT mice, but not in *Bgn* KO mice. (A) Total GAGs amount from mineralized (left panel) and non-mineralized (right panel) compartments of saline or CS injected WT mice bone matrix was quantified by DMMB assay. (B) After saline or CS injection, the amount of bound water in WT mice bone matrix was measured by low-field NMR, and normalized by comparing to saline controls. (C) Tissue-level toughness of femur mid-diaphysis from saline or CS injected WT mice was determined by nanoscratch test. (D) Total BMD was measured by DXA analysis at pre-injection and after injection with saline or CS. Total BMD change was obtained by calculating the ratio of total BMD before and after injection, and then normalized by comparing to saline controls. (E-H) The total GAGs amount, bound water, tissue-level toughness, and normalized BMD change were analyzed in *Bgn* KO mice after injection of saline or CS. n =5-9. * $p < 0.05$.

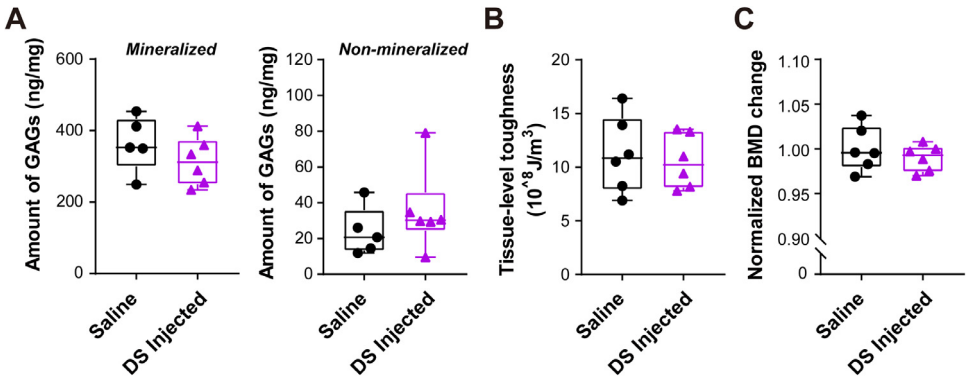

Fig. 5. Supplementation of dermatan sulfate did not change the GAGs amount, bone mineral density (BMD) in WT mice. (A) Total GAGs amount from mineralized (left panel) and non-mineralized (right panel) compartments of saline or DS injected WT matrix was quantified by DMMB assay. (B) Total BMD was measured by DXA analysis at pre-injection and after injection with saline or DS. Total BMD change was obtained by calculating the ratio of total BMD before and after injection, and then normalized by comparing to saline controls. (C) Tissue-level toughness of femur mid-diaphysis from saline or dermatan sulfate injected WT mice was determined by nanoscratch test. n =5-6.

Since dermatan sulfate (DS) is another major type of GAGs and has been shown to attach to Bgn core protein, we administrated DS (United States pharmacopeia reference standard) in middle-aged WT mice adopting the same strategy for supplementing CS. The results showed that the total amount of GAGs did not change in both mineralized and non-mineralized bone matrix after DS injection (Fig. 5A). In addition, the whole body BMD and tissue-level toughness did not show any significant difference between DS injected WT mice and saline controls (Fig. 5B and C). Together, these results suggest that administration of CS may increases the amount of GAGs and bound water in bone matrix, BMD, and tissue-level toughness of bone in WT mice, but this increase was not shown in *Bgn* KO and DS supplemented WT mice.

Chondroitin sulfate supplement inhibits osteoclast activation in WT mice, but not in *Bgn* KO mice

To further investigate the bone phenotypes of CS or saline injected WT and *Bgn* KO mice, we performed tartrate-resistant acid phosphatase (TRAP) staining for osteoclastogenesis analysis. The osteoclasts were visualized and quantified in endocortical femoral bones. The results showed that supplementation of CS significantly attenuated osteoclast activation in WT mice (Fig. 6), showing reduced osteoclast surface (Oc.S) normalized to bone surface (Oc.S/B.S) compared to saline group, while no difference was observed in *Bgn* KO mice.

In addition, bone dynamic histomorphometry parameters were analyzed using a calcein and

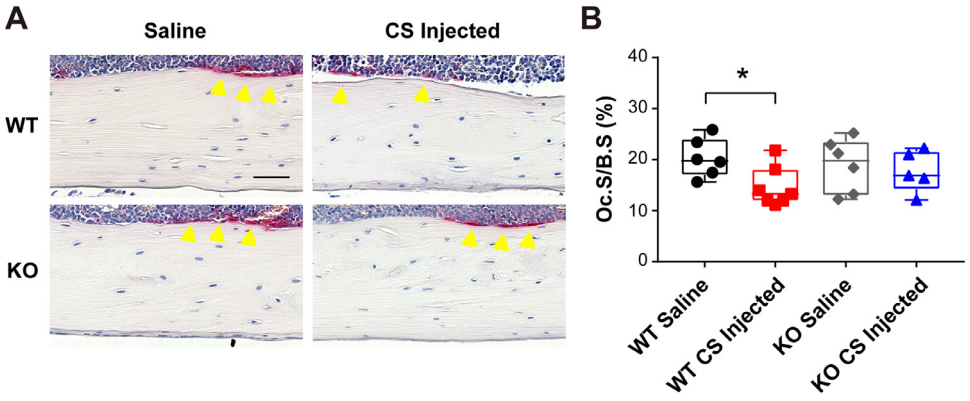

Fig. 6. Chondroitin sulfate injection decreased osteoclast surface in endocortical bone of WT mice. (A) Representative images of TRAP stained paraffin sections from WT and *Bgn* KO mice femoral bones after saline or CS injection. Yellow arrow heads indicate TRAP positive osteoclasts. Scale bar, 50 μm. (B) Quantification of Oc.S/B.S in saline or CS injected WT and *Bgn* KO mice bones. n =5-7. * $p < 0.05$. B.S, bone surface; OC.S, osteoclast surface; TRAP, tartrate-resistant acid phosphatase.

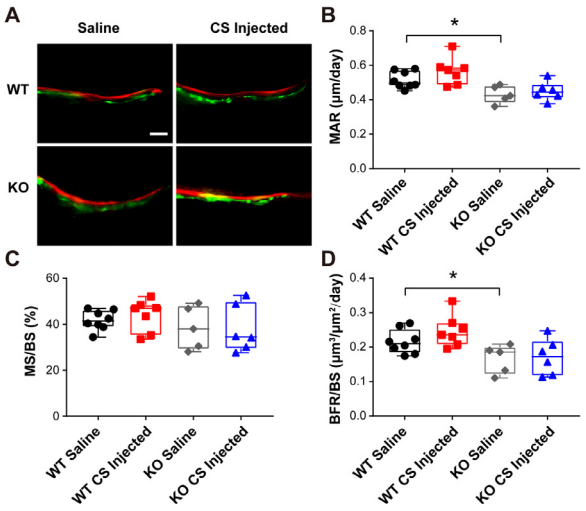

Fig. 7. Supplementation of chondroitin sulfate did not change bone dynamic histomorphometry parameters in endocortical bone of WT and *Bgn* KO mice. (A) Representative images of plastic sections prepared from CS or saline injected WT and *Bgn* KO mice. Scale bar = 50 μm. Mice were injected twice with calcein and alizarin red S dyes for dynamic histomorphometry. (B-D) Endocortical MAR, MS/BS, and BFR/BS were measured in unstained sections from the femoral mid-diaphysis. * $p < 0.05$. n = 5-8. MAR, mineral apposition rate; BFR, bone formation rate; BS, bone surface; MS, mineralizing surface.

alizarin double labeling assay. As shown in Fig. 7, the endocortical bone mineral apposition rate (MAR) and bone formation rate (BFR/BS) of saline injected *Bgn* KO mice were decreased compared to WT saline group, which is consistent with a previous report showing inhibited bone formation in *Bgn* KO mice [32]. However, compare to saline group, minimal effects of CS on bone formation were exhibited in WT and *Bgn* KO mice. These results suggested the anti-catabolic function of CS supplementation in WT mouse bone.

Discussion

Hydration status significantly affects bone strength and toughness. Synchrotron X-ray scattering and other studies show that the nanomechanics of bone is significantly dependent on the bound water in bone matrix and that the bound water residing in small ultrastructural spaces (< 4.0Å) dictates the mechanical behavior of bone by altering the interaction among hydroxyapatite (HA) crystals and their surrounding matrix [20,37]. Recent evidence indicates that PG/GAGs in the organic interface of extrafibrillar matrix may impart toughness to bone by attracting and retaining water in the matrix [24,25]. However, the key PG/GAGs involved in this process remained unidentified. In this study, using the *Bgn*-deficiency mouse model, we found that Bgn and CS, which are major components of PGs and GAGs in the extrafibrillar matrix of bone, respectively, played a pivotal role in the regulation of tissue-level hydration status and toughness of bone. This finding supports the hypothesis that PG/GAGs help attracting water into the organic interface between mineral crystallites, thus facilitating the ductile deformation of bone (Fig. 8).

The unreliable prediction of bone fracture by using BMD alone has raised the necessity of elucidating the ultrastructural and molecular origins of bone fragility in order to better predict and prevent bone fragility fractures. Previous studies have shown that water plays a critical role in sustaining the toughness of bone [37–39]. In addition to Type I collagen that constitutes 90% of organic phase and serves as a major site in bone that retains bound water, NCPs also possess a great capacity to attract water. Among NCPs, GAGs of PGs are highly electrically charged carbohydrate chains and interact with each other in a head to tail manner, forming interfibrillar supramolecular assemblies that could absorb water into the extracellular matrix of bone [40]. The contribution of PGs and GAGs to mechanical behavior of connective tissues, particularly soft tissues, such as tendon, articular cartilage and intervertebral disks, has been well documented [41–46]. However, the contribution of PGs to the mechanical behavior of mineralized tissues remains largely elusive. At the microscale, PGs may regulate the hydrostatic and osmotic potential, as well as poroelastic behavior of dentine and bone [23,47]. Our previous studies indicated the coupling effect of water and PGs on the toughness of bone by removing N-linked oligosaccharides enzymatically from the bone matrix *in vitro* [25]. In addition, Ho *et al* reported in an *in vitro* study that the removal of GAGs decreased the hardness and elastic modulus of cementum-dentin junction [48]. Moreover, the age-related loss of GAGs was reported to associate with the deterioration of bone toughness and the decreased amount of Bgn using an *ex vivo* model [24]. The results of this *in vivo* study again verify the previous findings, showing that PGs is coupled with bound water to toughen bone matrix by imparting ductility to the tissue.

As a member of the SLRPs family, Bgn is distributed abundantly throughout the cortical and trabecular bone matrix [49]. SLRPs play crucial roles in bone formation by regulating cell proliferation, matrix deposition and remodeling [50–54]. A *Bgn* deficient mouse model was first described by Xu *et al*, (1998) exhibiting age-dependent osteopenia compared to WT counterparts [32]. Disruption of *Bgn* also leads to structural abnormalities in bone collagen fibrils and metabolic defects in BMSCs [33,34,55]. Subsequent investigations identified that Bgn binds TGF-β and controls its bioactivity [56,57], modulates BMP4-induced osteoblast differentiation [58], and affects the Wnt signaling pathway [59]. The four-

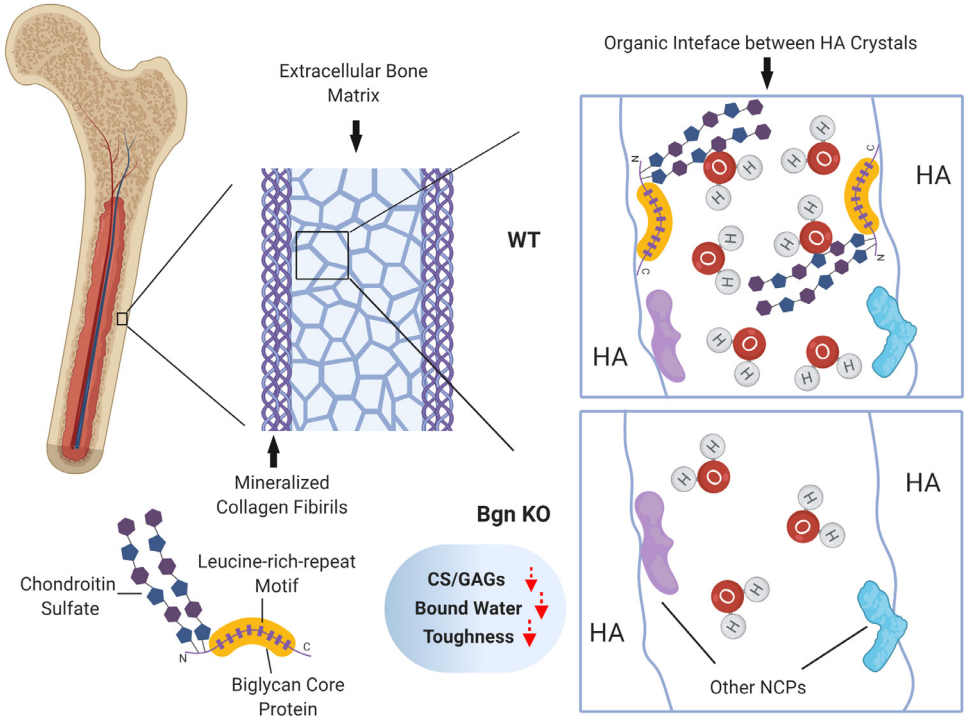

Fig. 8. Schematic summary of the role of Bgn and CS in water retention in extracellular bone matrix and bone toughness. Structurally, bone is comprised of mineralized collagen fibrils embedded in bone extrafibrillar matrix. These mineral crystals are bounded through organic interface of non-collagenous proteins and bound water. Bgn belongs to small leucine-rich proteoglycans with two sulfate chains and has a great potential to absorb water into the matrix. With deficiency of *Bgn* in knockout mouse model, there was a decreased amount of CS, total GAGs and bound water in bone matrix, along with the compromised bone toughness due to impaired water retention capability.

point bending test of *Bgn* KO mice bone showed reduced failure load and yield energy after 6 months of tissue development [32]. In this study, the nanoscratch test exhibited decreased tissue-level toughness of bone for 6-month-old *Bgn* deficiency mice, which is in good agreement with the impaired strength and ductility observed in the previous study, indicating the correlation of tissue-level and bulk mechanical properties. These results provided direct evidence for the mechanical contribution of PGs/GAGs in bone tissue.

Comprising about 20% of the volume, water is a key determinant of the mechanical behavior of bone, showing that loss of bound water correlates strongly with bone toughness deterioration [38,39,60]. Similarly, this study also showed a significant reduction of tissue-level toughness of bone in WT mice after removal of bound water, whereas such changes induced by removal of bound water were significantly reduced in *Bgn* KO mice. Under the dehydrated condition, the tissue-level toughness of bone is consistent between *Bgn* KO mice and WT controls. The results suggest that the coupling effect of water and PGs in sustaining the toughness of bone is disrupted once Bgn is removed from the matrix. However, it is noteworthy that the effect of bound water on the tissue-level toughness of bone still exists in *Bgn* KO mice, raising the possibility of the involvement of other PGs or non-PG factors in this process.

Bgn and decorin (Dcn) are considered as major PGs in the mineralized bone matrix. They share 57% identity at the amino acid level and are co-expressed in bone [29,30]. The studies of *Dcn*/*Bgn* double KO mice show that the skin tissue is much thinner and fragile than either single *Bgn* KO or single *Dcn* KO animals, and the osteopenia of the double KO mice is also more severe than the single *Bgn* KO mice [33,61]. Furthermore, Dcn protein level is higher in *Bgn* deficient tissues [62]. In osteoblasts with *Bgn* KO, Dcn accumulated to higher levels and localized unevenly in the extracellular matrix compared to the WT cell cultures [58]. These previous reports suggest a potential compensation and synergistic function between Bgn and Dcn [63]. Moreover, a recent report indicates that Bgn and another SLRPs, fibromodulin, are novel coupling components regulating osteoclastogenesis [64]. Since only *Bgn* KO mice were used in this study, it is possible that Dcn would replace some functions of Bgn to compensate the loss of structural integrity of bone matrix induced by *Bgn* depletion. Therefore, it

is anticipated that depletion of both *Bgn* and *Dcn* would result in much larger changes in bone mechanical properties.

Both Bgn and Dcn contain CS or DS side chains, and the attachment of CS versus DS is tissue-specific [53]. Classically, CS is predominantly attached to Bgn and Dcn within mineralized tissues, such as dentine and bone, whereas DS is mainly associated with soft connective tissues [50]. The agarose electrophoresis results of this study indicated that only CS appeared in mouse bone matrix, without noticeable presence of HS and DS. This observation implies that CS is the major GAGs in mouse bone matrix, although the minor presence of other GAGs still cannot be excluded.

The supplementation of CS to WT mice appeared to increase the total amount of GAGs and bound water in bone matrix, the whole body BMD, and the tissue-level toughness of bone. However, CS administration did not improve the mechanical properties of bone of *Bgn* KO mice. On the other hand, the DS supplementation seemed to have little effects on bone in the WT mice, which again underscores the predominant function of CS in bone matrix. In addition, bone histomophormetry studies indicated the decreased catabolic response in CS injected WT mice revealed by inhibited osteoclastogenesis, resulting in the net bone increase.

Previous study by Chen *et al* reports that *Bgn* deficiency blunts BMP-4 induced osteoblast differentiation *in vitro* [58]. The absence of Bgn decreases BMP-4 sensitivity caused by less BMP-4 binding, and is completely rescued by viral transfection of *Bgn*. A later study further highlights the importance of GAG chains of Bgn in modulating osteoblast differentiation, showing the expression of a mutant *Bgn* lacking GAGs binding sites cannot rescue the differentiation deficiency [65]. In contrast to the inhibition of osteoblastogenesis, *Bgn* KO mice did not show any difference in bone resorption compared to WT mice, which has been reported in previous study [32] and was also observed in our results. However, it is interesting to note that *Bgn* KO exacerbates LPS induced osteolysis and bone resorption *in vivo* [66]. *In vitro* co-culture of osteoblasts and osteoclasts shows that *Bgn* deficiency increases osteoclast differentiation through its effect on osteoblasts.

In our study, *Bgn* KO mice did not respond to CS injection induced GAGs elevation in bone matrix, which was probably attributable to less binding of CS under the condition of *Bgn* deficiency. Considering the role of highly negatively charged GAGs in retaining bound water, lack of increase in GAGs amount led to blunted bound water and thus reduced bone toughness. However, the direct evidence of CS binding ability under *Bgn* KO condition remains to be further investigated. In addition, since bone mass is maintained by a balance between bone formation and bone resorption, the lack of response to CS induced anti-catabolic effects may be due to the defective osteoblasts in *Bgn* KO mice. The results of this study demonstrate the pivotal role of Bgn and CS in bone toughness and homeostasis.

The anti-catabolic function of CS has been demonstrated in both chondrocytes and osteoblasts [67–69]. CS upregulated OPG production, while reduced RANKL expression, leading to a significantly higher OPG/RANKL ratio, which could exert a positive outcome for bone. Additionally, CS has direct function on osteoclasts, showing inhibition of osteoclast differentiation, and osteoclast-specific expression of TRAP and cathepsin K [70,71]. A recent *in vivo* study using CS treatment for diabetic osteoporosis reveals the increased bone-mineral density, repaired bone morphology and decreased femoral osteoclasts [72], which is in good agreement with our findings.

In fact, Bgn could serve as a potential therapeutic target, and administration of CS, possibly locally, may be a viable treatment strategy for osteoporosis and fracture healing. For instance, previous evidence shows that modulation of *Bgn* gene expression may counteract bone loss under an estrogen depletion condition [73]. Interestingly, oral administration of GAGs as nutritional supplements is controversial. CS has been widely consumed orally as a nutraceutical with applications in the therapy of osteoarthritis, which is mostly administered at doses ranging from 800 to 1200mg/day [74]. However, CS can be rapidly absorbed by the gastrointestinal system, with the overall bioavailability of CS ranges from 10% to 20% following oral administration [75,76]. Additionally, most of the absorbed CS reaches the blood compartment as depolarized low-molecular weight derivatives [77]. Our study used intradermal injection for CS administration, which could avoid the extensive first pass metabolism in the gastrointestinal tract prior to systemic availability, thus resulting in a much higher plasma concentration as shown in the previous studies using intravenously injection of CS [78].

In conclusion, our findings indicated that *Bgn* deficiency would lead to loss of CS, GAGs, and bound water in bone matrix, thus leading to the deterioration of the tissue-level toughness of bone. In addition, CS supplementation showed a potential in improving the toughness of bone, thus opening an additional avenue for developing new therapeutics in improving bone quality.

Materials and methods

Animals

The *Bgn* KO mice were originally generated by homologous recombination in embryonic stem cells as described elsewhere [32] and were generously

provided by Marian F. Young (National Institutes of Health, Bethesda, MD, USA). All experiments were performed using age-matched WT ($Bgn^{+/0}$, *Bgn* is on X chromosome) and *Bgn* deficient ($Bgn^{-/0}$) male mice, since *Bgn* deficiency, shows a minor effect on bone metabolism in female mice [73]. The genotype of the WT and *Bgn* KO mice was determined by a PCR-based assay [33]. The generated DNA fragments of 212 bp and 310 bp represent the WT and targeted *Bgn* allele, respectively.

For chondroitin sulfate (CS) supplementation experiments, 10 to 11-month-old WT and *Bgn* KO male mice were injected intradermally at the base of the tail with 4 mg/kg CS (Y0000280, Sigma-Aldrich, St. Louis, MO, USA) dissolved in saline and filtered. Control mice were injected with the same volume saline. Injections were given once a week for four weeks. All mice used were of C57BL/6 background. The mice were housed in a temperature-controlled room with a light/dark cycle of 12 hours at the UTHSCSA Institutional Lab Animal Research (LAR) facility, under specific pathogen-free conditions. Food and water were provided *ad libitum*. All animal protocols were performed in accordance with the National Institutes of Health guidelines for care and use of laboratory animals. The animal protocols were approved by the UTHSCSA Institutional Animal Care and Use Committee.

Extraction and quantification of glycosaminoglycans from bone tissues

The long bones (e.g. femur, tibia, humerus, and radius) were isolated free of soft tissues and bone marrow was removed by flushing with cold PBS by drilling a hole on both ends of the bones. GAGs were isolated from the non-mineralized (e.g., osteoids, membranes, and bone surfaces) and mineralized compartments in bone matrix, respectively [79–81]. Briefly, cortical bone tissues were crushed to fine powders with the pestle in a mortar filled with liquid nitrogen. The bone powders were first treated in lysis buffer I (4 M guanidine HCl, 0.05 M Tris, and 0.1 M 6-aminocaproic acid, pH 7.4) containing proteinase inhibitors at 4°C on the orbital shaker for 72 hours to remove GAGs from the non-mineralized compartment of bone. The carefully rinsed bone powders were treated in lysis buffer II (4 M guanidine HCl, 0.5 M EDTA tetrasodium salt, 0.05 M Tris, and 0.1 M 6-aminocaproic acid, pH 7.4) containing proteinase inhibitors at 4°C on the orbital shaker for 72 hours to remove GAGs from the mineralized compartment of bone. The supernatant from each treatment was collected and the amount of GAGs was quantified by dimethylmethylene blue (DMMB) assay as follows: 50 μL samples and 200 mL DMMB mix (46 mM DMMB (Sigma-Aldrich, St. Louis, MO, USA), 40 mM NaCl, and 40 mM glycine, pH adjusted to 3.0 with acetic acid). The above solution was pipetted into 96-well plates and shake for 5 seconds. The absorbance was recorded at wavelength 525 nm. The amount of GAGs was determined by comparing with the standard curves generated using purified GAGs (Sigma-Aldrich, St. Louis, MO, USA).

Chondroitinase ABC digestion of glycosaminoglycans

Chondroitinase ABC from *Proteus vulgaris* (C3667, Sigma-Aldrich, St. Louis, MO, USA) were reconstituted in 0.01% bovine serum albumin aqueous solution. The extracted GAG samples were incubated in 1 U/mL chondroitin ABC lyase or MilliQ water in freshly prepared digestion buffer (50 mM Tris, pH 8.0, 60 mM sodium acetate and 0.02% bovine serum albumin) overnight at 37°C. Digestion control samples: heparin sulfates (HS), dermatan sulfates (DS) and chondroitin sulfates (CS) extracted from shark cartilage (1 μg/μL) were incubated in chondroitin ABC lyase or MilliQ water overnight at 37°C and digested samples were analyzed by agarose gel electrophoresis.

Agarose gel electrophoresis

GAGs isolated from non-mineralized and mineralized bone samples as well as GAGs standards, HS, DS and CS were separated by 0.9% agarose gel electrophoresis in 1,3-propanediamine acetate buffer (50 mM, pH 9.0) for 90 min at 80V. Following the electrophoresis, the GAGs were fixed using 0.2% (w/v) cetyl-trimethyl-ammonium bromide (CTAB) solution for 1 hour at room temperature, and then the gels were dried. Gels were stained with 0.1% (w/v) toluidine blue prepared in solution of 50% (v/v) ethanol, 49% (v/v) water and 1% (v/v) water, and destained in the same solution without toluidine blue.

Western blotting

Protein concentrations of proteoglycans extracted from mineralized matrix of mice cortical bone samples were determined by Micro BCA Protein Kit (Thermo Scientific, Rockford, IL, USA). Equal amount of proteins determined by microBCA assay was treated with or without Protein Deglycosylation Enzyme mix (P6044, New England Biolabs, MA, USA) for 1 hour at 37°C following the manufacturer's instructions. Protein Deglycosylation Enzyme Mix contains PNGase F, O-glycosidase, neuraminidase, β1-4-galactosidase, and β-Nacetylglucosaminidase, which can completely remove glycosylation. Each protein sample was boiled in SDS loading buffer, subjected to 10% SDS-polyacrylamide gel electrophoresis, and electroblotted onto a nitrocellulose membrane. Membranes were incubated with a 1:500 dilution of

polyclonal anti-Bgn (LF-159) antibody (#ENH020-FP, Kerafast, Boston, USA). Primary antibodies were detected with HRP-conjugated anti-goat secondary antibody and were developed using an ECL kit (Amersham Biosciences, Piscataway, NJ, USA).

Immunohistochemistry staining

The avidin-biotin-peroxidase complex (ABC) Immunostaining Assay Kit (PK-6101, Vector Laboratories, Burlingame, CA) was used as previously described [82]. Paraffin sections of bone tissue were deparaffinized and rehydrated to unmask antigens using sodium citrate buffer (pH 6.0) at 65°C for 2 hours for Bgn staining. Bone tissue sections were enzymatically digested with chondroitinase ABC at 37°C for 1 hour before treated with goat normal serum for 20 minutes at room temperature to block non-specific background staining. The sections were stained with anti-Bgn (LF-159) antibody (#ENH020-FP, Kerafast, Boston, USA) at 1:100 dilution overnight at 4°C, followed by incubation with biotin-labeled secondary antibody and ABC Reagent for 30 minutes. Samples were washed in PBS buffer and developed in DAB (SK4100) chromogen solution (Vector Laboratories). Tissues were then counterstained with VECTOR Hematoxylin (H-3401) for 2 minutes at room temperature and mounted. Sections were photographed using the Keyence microscope (BZ-X710, Keyence, Osaka, Japan).

Alcian blue staining

For preparation of paraffin tissue sections, the femoral and tibial bones from 6-month-old male mice were fixed in 4% paraformaldehyde for 2 days prior to decalcification with 10% EDTA (pH 7.4) for 4 weeks. The samples were embedded in paraffin and 5 μm thick sections were cut onto glass slides and stained with Alcian blue. Alcian blue staining is a semiquantitative method to measure GAG contents [83,84]. Bone sections were incubated in 3% acetic acid for 3 minutes and then incubated in 1% Alcian blue 8GX (Sigma-Aldrich, St. Louis, MO, USA), pH 2.5, for 40 min at room temperature followed by destaining in water and counterstained with Nuclear Fast Red (N3020 Sigma-Aldrich, St. Louis, MO, USA).

Low-energy NMR measurement of bound water in bone matrix

The bound water was measured using a low-field NMR technique. Based on the T_2 relaxation information, the relative amount of freely mobile water, bound water, and lattice water was assessed. Briefly, a low-field NMR spectrometer (Bruker 20 MHz) was configured at a proton frequency of 20 MHz to assess the amount of bound water using bone powders from the animal models. 1H spin−spin (T_2) relaxation profiles were obtained using the NMR CPMG, {90° [−τ − 180° − τ (echo)]n − TR} spin echo method, which has a 9.5 μs wide RF-90° pulse, τ of 1000μs, and TR (sequence repetition rate) of 15s. One thousand echoes were recorded (one scan with n=1000) to obtain the T_2 profile, with 64 scans used for the measurements. The FID signal was sampled and recorded at 2 μs intervals using a 9.5μs wide 90° RF-pulse for bound water measurements. For each FID profile, 1500 data points were acquired in one scan (an approximate 3ms delay window). An inversion relaxation technique was used to invert both CPMG and FID data to a T_2 relaxation distribution spectrum. The relative amount of bound water was then estimated as the ratio of the total intensity of bound water signal with respect to the total intensity of the solid form water signal (representative of bone mass) of each sample.

Measurement of the tissue level toughness of bone using a nanoscratch test

One femur from each mouse was freshly embedded in the plastic resin (PMMA) and the cross-section of the mid-diaphysis was cut, polished, and mounted on a custom designed specimen holder. The average surface roughness was kept less than 80 nm. For the nanoscratch test under wet condition, a lateral hole was drilled in the embedded specimen and PBS solution in the chamber would fill in the intra-medullar cavity of the femurs, thus making the bone specimens wet throughout the testing process. For nanoscratch test under dry condition, bone specimens were dehydrated in a vacuum oven at 70°C for 4 hours prior to the test to remove mobile and bound water in the tissue [9]. The nanoscratch tests were performed on a Nano Indenter XP system (Keysight Technologies, Santa Rosa, CA, USA) with a cube corner diamond tip as described previously [85,86]. A constant penetration load was set at 5 mN and the scratch length was set at 20 μm. Test locations were randomly chosen in the middle cortex of each specimen under a microscope attached to the system. During the scratching, the cross-profile of the scratch groove was measured to estimate the width of the scratch groove. The tissue level toughness of bone was estimated using the following equation,

$$u_s = \frac{F_t L}{V} = \frac{F_t}{A}$$

where, u_s is the nanoscratch toughness, F_t is the lateral scratch force, L is the scratch length, V is the volume of the scratch groove, and A is the average cross-sectional area of the scratch groove. The average of six measurements was used as the tissue level toughness of each bone specimen.

Bone mineral density (BMD) measurement

Mice were anesthetized by intraperitoneal injection of 100 mg/kg of ketamine (Butler Schein, Dublin, OH, USA) and 16 mg/kg of xylazine (Butler Schein). We used a dual-energy X-ray absorptiometry (DEXA) scanner, Lunar PIXImus Densitometer (GE Medical Systems, Piscataway, NJ, USA) to measure the BMD at pre-injection and after saline or chondroitin sulfate injection. The BMD values of the total bones were acquired.

Bone TRAP staining for osteoclasts

Tissue sections were stained with tartrate-resistant acid phosphatase (TRAP) using Leukocyte Acid Phosphatase Staining Kit (Sigma) according to the manufacturer's protocols. The NIH Image J software was used to quantify osteoclast surface (Oc.S) and bone surface (BS) along the endocortical surface in the femur midshaft. The Oc.S/B.S value was then calculated.

Calcein and alizarin labeling, and dynamic bone histomorphometry

Two weeks after first CS or saline injection, the mice were subjected to an intraperitoneal injection of calcein (Sigma) at 20 mg/kg body weight, followed by an alizarin red S (Sigma) injection at 30 mg/kg body weight 12 days later. Three days after the second injection, the mice were euthanized, and femurs and tibias were dissected and embedded undecalcified in methylmethacrylate for plastic tissue sectioning. The embedded samples were cut to 8 μm thickness tissue sections by a skiving machine (Leica RM2265). Sections were photographed using a Keyence microscope (BZ-X710, Keyence, Osaka, Japan). The following bone parameters were quantified in the endocortical regions with Image J software: total perimeter (BS), single label perimeter (sLS), double label perimeter (dLS), and distance between labels (Ir.L.Th). The following values were then calculated: mineralizing surface (MS/BS= [sLS/2+dLS]/BS), mineral apposition rate (MAR = Ir.L.Th /10), and bone formation rate (BFR/BS = MAR_ (sLS/2+dLS)/BS).

Statistical analysis

Statistical analysis was performed using GraphPad Prism5 statistics software (GraphPad). T-test and Two-way ANOVA with *post hoc* Tukey test was used for statistical analysis. Asterisks indicate the degree of significant differences compared with the controls, *, $P < 0.05$; **, $P < 0.01$; ***, $P < 0.001$.

Declaration of Competing Interest

The authors declare no competing interests.

Acknowledgments

The authors thank Dr. Marian Young at the National Institute of Dental and Craniofacial Research, National Institutes of Health for generously providing biglycan knockout mice, Hongyun Cheng for techical assistance and Eduardo R. Cardenas for critical reading of the manuscript. The work was supported by NIH grants, AR076190 to X.W and J.X.J and Welch Foundation grant AQ-1507 to J.X.J.

Received 7 May 2020;
Received in revised form 23 September 2020;
Accepted 23 September 2020
Available online 28 September 2020

Keywords:
Biglycan;
Chondroitin sulfate;
Bone matrix;
Bone toughness;
Bound water

References

[1] A. Alho, T. Husby, A. Hoiseth, Bone mineral content and mechanical strength. An ex vivo study on human femora at autopsy, Clin. Orthopaed. Relat. Res. 227 (1988) 292–297.
[2] T.J. Aspray, A. Prentice, T.J. Cole, Y. Sawo, J. Reeve, R.M. Francis, Low bone mineral content is common but osteoporotic fractures are rare in elderly rural Gambian women, J. Bone miner. Res. 11 (7) (1996) 1019–1025 the official J. the American Society for Bone and Mineral Research.
[3] S.L. Hui, C.W. Slemenda, C.C. Johnston Jr., Age and bone mass as predictors of fracture in a prospective study, J. Clin. Invest. 81 (6) (1988) 1804–1809.
[4] R.W. McCalden, J.A. McGeough, M.B. Barker, C.M. Court-Brown, Age-related changes in the tensile properties of cortical bone. The relative importance of changes in porosity, mineralization, and microstructure, J. Bone Joint surg. Am. 75 (8) (1993) 1193–1205.
[5] S. Weiner, W. Traub, Bone structure: from angstroms to microns, FASEB J. 6 (3) (1992) 879–885 official publication of the Federation of American Societies for Experimental Biology.
[6] R.K. Nalla, J.H. Kinney, R.O. Ritchie, Effect of orientation on the in vitro fracture toughness of dentin: the role of toughening mechanisms, Biomaterials 24 (22) (2003) 3955–3968.
[7] X. Wang, X. Shen, X. Li, C.M. Agrawal, Age-related changes in the collagen network and toughness of bone, Bone 31 (1) (2002) 1–7.

[8] D.B. Burr, Bone material properties and mineral matrix contributions to fracture risk or age in women and men, J. Musculoskeletal Neuronal Interact. 2 (3) (2002) 201–204.
[9] X. Wang, R.A. Bank, J.M. TeKoppele, C.M. Agrawal, The role of collagen in determining bone mechanical properties, J. Orthopaed. Res. 19 (6) (2001) 1021–1026 official publication of the Orthopaedic Research Society.
[10] J.D. Currey, Effects of differences in mineralization on the mechanical properties of bone, Philos. Trans. R. Soc. Lond. Ser. B, Biol. Sci. 304 (1121) (1984) 509–518.
[11] O.L. Katsamenis, H.M. Chong, O.G. Andriotis, P.J. Thurner, Load-bearing in cortical bone microstructure: Selective stiffening and heterogeneous strain distribution at the lamellar level, J. Mech. Behav. Biomed. Mater. 17 (2013) 152–165.
[12] G.E. Sroga, D. Vashishth, Effects of bone matrix proteins on fracture and fragility in osteoporosis, Current Osteoporosis Rep. 10 (2) (2012) 141–150.
[13] M. Unal, F. Cingoz, C. Bagcioglu, Y. Sozer, O. Akkus, Interrelationships between electrical, mechanical and hydration properties of cortical bone, J. Mech. Behav. Biomed. Mater. 77 (2018) 12–23.
[14] S.M. Best, M.J. Duer, D.G. Reid, E.R. Wise, S. Zou, Towards a model of the mineral-organic interface in bone: NMR of the structure of synthetic glycosaminoglycan- and polyaspartate-calcium phosphate composites, Magn. Resonance Chem. MRC 46 (4) (2008) 323–329.
[15] Y. Hashimoto, G.E. Lester, B. Caterson, M. Yamauchi, EDTA-insoluble, calcium-binding proteoglycan in bovine bone, Calcified Tissue Int. 56 (5) (1995) 398–402.
[16] R.V. Iozzo, L. Schaefer, Proteoglycan form and function: A comprehensive nomenclature of proteoglycans, Matrix Biol. J. Int. Soc. Matrix Biol. 42 (2015) 11–55.
[17] J.J. Broz, S.J. Simske, A.R. Greenberg, M.W. Luttges, Effects of rehydration state on the flexural properties of whole mouse long bones, J. Biomech. Eng. 115 (4A) (1993) 447–449.
[18] M.W. Jameson, J.A. Hood, B.G. Tidmarsh, The effects of dehydration and rehydration on some mechanical properties of human dentine, J. Biomech. 26 (9) (1993) 1055–1065.
[19] J.S. Nyman, A. Roy, X. Shen, R.L. Acuna, J.H. Tyler, X. Wang, The influence of water removal on the strength and toughness of cortical bone, J. Biomech. 39 (5) (2006) 931–938.
[20] J. Samuel, D. Sinha, J.C. Zhao, X. Wang, Water residing in small ultrastructural spaces plays a critical role in the mechanical behavior of bone, Bone 59 (2014) 199–206.
[21] P. Zhu, J. Xu, N. Sahar, M.D. Morris, D.H. Kohn, A. Ramamoorthy, Time-resolved dehydration-induced structural changes in an intact bovine cortical bone revealed by solid-state NMR spectroscopy, J. Am. Chem. Soc. 131 (47) (2009) 17064–17065.
[22] A. Salustri, L. Campagnolo, F.G. Klinger, A. Camaioni, Molecular organization and mechanical properties of the hyaluronan matrix surrounding the mammalian oocyte, Matrix Biol. J. Int. Soc. Matrix Biol. 78-79 (2019) 11–23.
[23] L.E. Bertassoni, M.V. Swain, The contribution of proteoglycans to the mechanical behavior of mineralized tissues, J. Mech. Behav. Biomed. Mater. 38 (2014) 91–104.
[24] X. Wang, R. Hua, A. Ahsan, Q. Ni, Y. Huang, S. Gu, J.X. Jiang, Age-related deterioration of bone toughness is related to diminishing amount of matrix glycosaminoglycans (Gags), JBMR Plus 2 (3) (2018) 164–173.
[25] X. Wang, H. Xu, Y. Huang, S. Gu, J.X. Jiang, Coupling effect of water and proteoglycans on the in situ toughness of bone, J. Bone Miner. Res. 31 (5) (2016) 1026–1029.
[26] L.W. Fisher, J.D. Termine, S.W. Dejter Jr, S.W. Whitson, M. Yanagishita, J.H. Kimura, V.C. Hascall, H.K. Kleinman, J.R. Hassell, B. Nilsson, Proteoglycans of developing bone, J. Biol. Chem. 258 (10) (1983) 6588–6594.
[27] L.W. Fisher, J.D. Termine, M.F. Young, Deduced protein sequence of bone small proteoglycan I (biglycan) shows homology with proteoglycan II (decorin) and several nonconnective tissue proteins in a variety of species, J. Biol. Chem. 264 (8) (1989) 4571–4576.
[28] P. Bianco, L.W. Fisher, M.F. Young, J.D. Termine, P.G. Robey, Expression and localization of the two small proteoglycans biglycan and decorin in developing human skeletal and non-skeletal tissues, J. Histochem. Cytochem. 38 (11) (1990) 1549–1563.
[29] R.V. Iozzo, The biology of the small leucine-rich proteoglycans. Functional network of interactive proteins, J. Biol. Chem. 274 (27) (1999) 18843–18846.
[30] R.V. Iozzo, The family of the small leucine-rich proteoglycans: key regulators of matrix assembly and cellular growth, Crit. Rev. Biochem. Mol. Biol. 32 (2) (1997) 141–174.
[31] K. Pietraszek-Gremplewicz, K. Karamanou, A. Niang, M. Dauchez, N. Belloy, F.X. Maquart, S. Baud, S. Brezillon, Small leucine-rich proteoglycans and matrix metalloproteinase-14: Key partners? Matrix Biol. J. Int. Soc. Matrix Biol. 75-76 (2019) 271–285.
[32] T. Xu, P. Bianco, L.W. Fisher, G. Longenecker, E. Smith, S. Goldstein, J. Bonadio, A. Boskey, A.M. Heegaard, B. Sommer, K. Satomura, P. Dominguez, C. Zhao, A.B. Kulkarni, P.G. Robey, M.F. Young, Targeted disruption of the biglycan gene leads to an osteoporosis-like phenotype in mice, Nat. Genet. 20 (1) (1998) 78–82.
[33] A. Corsi, T. Xu, X.D. Chen, A. Boyde, J. Liang, M. Mankani, B. Sommer, R.V. Iozzo, I. Eichstetter, P.G. Robey, P. Bianco, M.F. Young, Phenotypic effects of biglycan deficiency are linked to collagen fibril abnormalities, are synergized by decorin deficiency, and mimic Ehlers-Danlos-like changes in bone and other connective tissues, J. Bone Miner. Res. 17 (7) (2002) 1180–1189.
[34] X.D. Chen, S. Shi, T. Xu, P.G. Robey, M.F. Young, Age-related osteoporosis in biglycan-deficient mice is related to defects in bone marrow stromal cells, J. Bone Miner. Res. 17 (2) (2002) 331–340.
[35] M.F. Young, Y. Bi, L. Ameye, T. Xu, S. Wadhwa, A. Heegaard, T. Kilts, X.D. Chen, Small leucine-rich proteoglycans in the aging skeleton, J. Musculoskeletal Neuronal Interact. 6 (4) (2006) 364–365.
[36] J.Y. Wang, M.H. Roehrl, Glycosaminoglycans are a potential cause of rheumatoid arthritis, Proc. Natl. Acad. Sci. USA 99 (22) (2002) 14362–14367.
[37] J. Samuel, J.S. Park, J. Almer, X. Wang, Effect of water on nanomechanics of bone is different between tension and compression, J. Mech. Behav. Biomed. Mater. 57 (2016) 128–138.
[38] M. Granke, M.D. Does, J.S. Nyman, The Role of Water Compartments in the Material Properties of Cortical Bone, Calcified Tissue Int. 97 (3) (2015) 292–307.
[39] J.S. Nyman, Q. Ni, D.P. Nicolella, X. Wang, Measurements of mobile and bound water by nuclear magnetic resonance correlate with mechanical properties of bone, Bone 42 (1) (2008) 193–199.
[40] N.S. Gandhi, R.L. Mancera, The structure of glycosaminoglycans and their interactions with proteins, Chem. Biol. Drug Des. 72 (6) (2008) 455–482.

[41] E.H. Han, S.S. Chen, S.M. Klisch, R.L. Sah, Contribution of proteoglycan osmotic swelling pressure to the compressive properties of articular cartilage, Biophys. J. 101 (4) (2011) 916–924.
[42] S. Sivan, Y. Merkher, E. Wachtel, S. Ehrlich, A. Maroudas, Correlation of swelling pressure and intrafibrillar water in young and aged human intervertebral discs, J. Orthopaed. Res. 24 (6) (2006) 1292–1298 official publication of the Orthopaedic Research Society.
[43] D.D. Sun, X.E. Guo, M. Likhitpanichkul, W.M. Lai, V.C. Mow, The influence of the fixed negative charges on mechanical and electrical behaviors of articular cartilage under unconfined compression, J. Biomech. Eng. 126 (1) (2004) 6–16.
[44] H. Yao, M.A. Justiz, D. Flagler, W.Y. Gu, Effects of swelling pressure and hydraulic permeability on dynamic compressive behavior of lumbar annulus fibrosus, Ann. Biomed. Eng. 30 (10) (2002) 1234–1241.
[45] J.E. Scott, A.M. Thomlinson, The structure of interfibrillar proteoglycan bridges (shape modules') in extracellular matrix of fibrous connective tissues and their stability in various chemical environments, J. Anatomy 192 (Pt 3) (1998) 391–405.
[46] K.A. Robinson, M. Sun, C.E. Barnum, S.N. Weiss, J. Huegel, S.S. Shetye, L. Lin, D. Saez, S.M. Adams, R.V. Iozzo, L.J. Soslowsky, D.E. Birk, Decorin and biglycan are necessary for maintaining collagen fibril structure, fiber realignment, and mechanical properties of mature tendons, Matrix Biol. J. Int. Soc. Matrix Biol. 64 (2017) 81–93.
[47] S. Morgan, A.A. Poundarik, D. Vashishth, Do non-collagenous proteins affect skeletal mechanical properties? Calcified Tissue Int. 97 (3) (2015) 281–291.
[48] S.P. Ho, R.M. Sulyanto, S.J. Marshall, G.W. Marshall, The cementum-dentin junction also contains glycosaminoglycans and collagen fibrils, J. Struct. Biol. 151 (1) (2005) 69–78.
[49] R.T. Ingram, B.L. Clarke, L.W. Fisher, L.A. Fitzpatrick, Distribution of noncollagenous proteins in the matrix of adult human bone: evidence of anatomic and functional heterogeneity, J. Bone Miner. Res. 8 (9) (1993) 1019–1029.
[50] R.J. Waddington, H.C. Roberts, R.V. Sugars, E. Schonherr, Differential roles for small leucine-rich proteoglycans in bone formation, Eur. Cells Mater. 6 (2003) 12–21 discussion 21.
[51] D. Parisuthiman, Y. Mochida, W.R. Duarte, M. Yamauchi, Biglycan modulates osteoblast differentiation and matrix mineralization, J. Bone Miner. Res. 20 (10) (2005) 1878–1886.
[52] L. Schaefer, R.V. Iozzo, Biological functions of the small leucine-rich proteoglycans: from genetics to signal transduction, J. Biol. Chem. 283 (31) (2008) 21305–21309.
[53] D. Nikitovic, J. Aggelidakis, M.F. Young, R.V. Iozzo, N.K. Karamanos, G.N. Tzanakakis, The biology of small leucine-rich proteoglycans in bone pathophysiology, J. Biol. Chem. 287 (41) (2012) 33926–33933.
[54] N.K. Karamanos, A.D. Theocharis, T. Neill, R.V. Iozzo, Matrix modeling and remodeling: A biological interplay regulating tissue homeostasis and diseases, Matrix Biol. J. Int. Soc. Matrix Biol. 75-76 (2019) 1–11.
[55] X.D. Chen, M.R. Allen, S. Bloomfield, T. Xu, M. Young, Biglycan-deficient mice have delayed osteogenesis after marrow ablation, Calcified Tissue Int. 72 (5) (2003) 577–582.
[56] A. Hildebrand, M. Romaris, L.M. Rasmussen, D. Heinegard, D.R. Twardzik, W.A. Border, E. Ruoslahti, Interaction of the small interstitial proteoglycans biglycan, decorin and fibromodulin with transforming growth factor beta, Biochem. J. 302 (Pt 2) (1994) 527–534.
[57] M. Kolb, P.J. Margetts, P.J. Sime, J. Gauldie, Proteoglycans decorin and biglycan differentially modulate TGF-beta-mediated fibrotic responses in the lung, Am. J. Physiol. Lung Cell. Mol. Physiol. 280 (6) (2001) L1327–L1334.
[58] X.D. Chen, L.W. Fisher, P.G. Robey, M.F. Young, The small leucine-rich proteoglycan biglycan modulates BMP-4-induced osteoblast differentiation, FASEB J. 18 (9) (2004) 948–958.
[59] A.D. Berendsen, L.W. Fisher, T.M. Kilts, R.T. Owens, P.G. Robey, J.S. Gutkind, M.F. Young, Modulation of canonical Wnt signaling by the extracellular matrix component biglycan, Proc. Natl. Acad. Sci. USA 108 (41) (2011) 17022–17027.
[60] M. Granke, A.J. Makowski, S. Uppuganti, M.D. Does, J.S. Nyman, Identifying novel clinical surrogates to assess human bone fracture toughness, J. Bone Miner. Res. 30 (7) (2015) 1290–1300.
[61] K.G. Danielson, H. Baribault, D.F. Holmes, H. Graham, K.E. Kadler, R.V. Iozzo, Targeted disruption of decorin leads to abnormal collagen fibril morphology and skin fragility, The J. Cell Biol. 136 (3) (1997) 729–743.
[62] M.F. Young, Y. Bi, L. Ameye, X.D. Chen, Biglycan knockout mice: new models for musculoskeletal diseases, Glycoconjugate J. 19 (4-5) (2002) 257–262.
[63] L. Ameye, M.F. Young, Mice deficient in small leucine-rich proteoglycans: novel in vivo models for osteoporosis, osteoarthritis, Ehlers-Danlos syndrome, muscular dystrophy, and corneal diseases, Glycobiology 12 (9) (2002) 107R–116R.
[64] V. Kram, T.M. Kilts, N. Bhattacharyya, L. Li, M.F. Young, Small leucine rich proteoglycans, a novel link to osteoclastogenesis, Sci. Rep. 7 (1) (2017) 12627.
[65] Y. Ye, W. Hu, F. Guo, W. Zhang, J. Wang, A. Chen, Glycosaminoglycan chains of biglycan promote bone morphogenetic protein-4-induced osteoblast differentiation, Int. J. Mol. Med. 30 (5) (2012) 1075–1080.
[66] Y. Bi, K.L. Nielsen, T.M. Kilts, A. Yoon, A.K. M, H.F. Wimer, E.M. Greenfield, A.M. Heegaard, M.F. Young, Biglycan deficiency increases osteoclast differentiation and activity due to defective osteoblasts, Bone 38 (6) (2006) 778–786.
[67] E. Pecchi, S. Priam, Z. Mladenovic, M. Gosset, A.S. Saurel, L. Aguilar, F. Berenbaum, C. Jacques, A potential role of chondroitin sulfate on bone in osteoarthritis: inhibition of prostaglandin E(2) and matrix metalloproteinases synthesis in interleukin-1beta-stimulated osteoblasts, Osteoarthrit. Cartil. 20 (2) (2012) 127–135.
[68] S.K. Tat, J.P. Pelletier, J. Verges, D. Lajeunesse, E. Montell, H. Fahmi, M. Lavigne, J. Martel-Pelletier, Chondroitin and glucosamine sulfate in combination decrease the pro-resorptive properties of human osteoarthritis subchondral bone osteoblasts: a basic science study, Arthritis Res. Ther. 9 (6) (2007) R117.
[69] J. Monfort, J.P. Pelletier, N. Garcia-Giralt, J. Martel-Pelletier, Biochemical basis of the effect of chondroitin sulphate on osteoarthritis articular tissues, Ann. Rheum. Dis. 67 (6) (2008) 735–740.
[70] J. Salbach, S. Kliemt, M. Rauner, T.D. Rachner, C. Goettsch, S. Kalkhof, M. von Bergen, S. Moller, M. Schnabelrauch, V. Hintze, D. Scharnweber, L.C. Hofbauer, The effect of the degree of sulfation of glycosaminoglycans on osteoclast function and signaling pathways, Biomaterials 33 (33) (2012) 8418–8429.
[71] T. Miyazaki, S. Miyauchi, T. Anada, A. Tawada, O. Suzuki, Chondroitin sulfate-E binds to both osteoactivin and integrin alphaVbeta3 and inhibits osteoclast differentiation, J. Cell. Biochem. 116 (10) (2015) 2247–2257.

[72] H.X. Zheng, J. Chen, Y.X. Zu, E.Z. Wang, S.S. Qi, Chondroitin sulfate prevents STZ Induced diabetic osteoporosis through decreasing blood glucose, antioxidative stress, anti-inflammation and OPG/RANKL expression regulation, Int. J. Mol. Sci. 21 (15) (2020).
[73] K.L. Nielsen, M.R. Allen, S.A. Bloomfield, T.L. Andersen, X.D. Chen, H.S. Poulsen, M.F. Young, A.M. Heegaard, Biglycan deficiency interferes with ovariectomy-induced bone loss, J. Bone Miner. Res. 18 (12) (2003) 2152–2158.
[74] Y. Henrotin, M. Mathy, C. Sanchez, C. Lambert, Chondroitin sulfate in the treatment of osteoarthritis: from in vitro studies to clinical recommendations, Ther. Adv. Musculoskeletal Dis. 2 (6) (2010) 335–348.
[75] R.M. Lauder, Chondroitin sulphate: a complex molecule with potential impacts on a wide range of biological systems, Complem. Ther. Med. 17 (1) (2009) 56–62.
[76] Y.H. Liau, N. Galicki, M.I. Horowitz, Degradation of chondroitin 4-sulfate by rat stomach exoglycosidases, sulfohydrolase and hyaluronidase-like enzymes, Digestion 21 (3) (1981) 117–124.
[77] S. Kusano, A. Ootani, S. Sakai, N. Igarashi, A. Takeguchi, H. Toyoda, T. Toida, HPLC determination of chondrosine in mouse blood plasma after intravenous or oral dose, Biol. Pharm. Bull. 30 (8) (2007) 1365–1368.
[78] J. Du, N. White, N.D. Eddington, The bioavailability and pharmacokinetics of glucosamine hydrochloride and chondroitin sulfate after oral and intravenous single dose administration in the horse, Biopharmaceut. Drug Disposit. 25 (3) (2004) 109–116.
[79] T.P. Cleland, K. Voegele, M.H. Schweitzer, Empirical evaluation of bone extraction protocols, PloS One 7 (2) (2012) e31443.
[80] A. Franzen, D. Heinegard, Extraction and purification of proteoglycans from mature bovine bone, Biochem. J. 224 (1) (1984) 47–58.
[81] M. Wendel, Y. Sommarin, D. Heinegard, Bone matrix proteins: isolation and characterization of a novel cell-binding keratan sulfate proteoglycan (osteoadherin) from bovine bone, J. Cell Biol. 141 (3) (1998) 839–847.
[82] L. Ma, R. Hua, Y. Tian, H. Cheng, R.J. Fajardo, J.J. Pearson, T. Guda, D.B. Shropshire, S. Gu, J.X. Jiang, Connexin 43 hemichannels protect bone loss during estrogen deficiency, Bone Res. 7 (2019) 11.
[83] R. Pacheco-Costa, J.R. Kadakia, E.G. Atkinson, J.M. Wallace, L.I. Plotkin, R.D. Reginato, Connexin37 deficiency alters organic bone matrix, cortical bone geometry, and increases Wnt/beta-catenin signaling, Bone 97 (2017) 105–113.
[84] H. Brisby, A.Q. Wei, T. Molloy, S.A. Chung, G.A. Murrell, A.D. Diwan, The effect of running exercise on intervertebral disc extracellular matrix production in a rat model, Spine 35 (15) (2010) 1429–1436.
[85] A. Islam, X. Neil Dong, X. Wang, Mechanistic modeling of a nanoscratch test for determination of in situ toughness of bone, J. Mech. Behav. Biomed. Mater. 5 (1) (2012) 156–164.
[86] X. Wang, Y.J. Yoon, H. Ji, A novel scratching approach for measuring age-related changes in the in situ toughness of bone, J. Biomech. 40 (6) (2007) 1401–1404.